

## Modeling and control of central air conditionings for providing regulation services for power systems

Kang Xie<sup>a</sup>, Hongxun Hui<sup>b,\*</sup>, Yi Ding<sup>a,\*</sup>, Yonghua Song<sup>b</sup>, Chengjin Ye<sup>a</sup>, Wandong Zheng<sup>c</sup>, Shuiquan Ye<sup>d</sup>

<sup>a</sup> College of Electrical Engineering, Zhejiang University, Hangzhou, China

<sup>b</sup> State Key Laboratory of Internet of Things for Smart City, University of Macau, Macau, China

<sup>c</sup> School of Environmental Science and Engineering, Tianjin University, Tianjin, China

<sup>d</sup> RunPaq Technology Co. Ltd, Hangzhou, China

### HIGHLIGHTS

- A quantitative assessment method of CACs' regulation capacity is proposed.
- An adaptive method is proposed to allocate regulation requirements among CACs.
- A fluctuation suppression control is adopted to guarantee the regulation accuracy.
- An online control method is developed to ensure occupants' comfortable temperatures.

### ARTICLE INFO

#### Keywords:

Central air conditioning  
Thermal-electrical model  
Quantitative assessment  
Control strategy  
Regulation services

### ABSTRACT

The increasing renewable energies bring more generation fluctuations to power systems, which puts forward a higher requirement on regulation services for maintaining the system balance. Existing traditional generating units probably cannot provide sufficient regulation services to solve this challenge. With the progress of information and communication technologies, it is possible to control demand-side flexible loads to provide regulation services. Among various flexible loads, central air conditionings (CACs) have huge regulation potential, because CACs account for about 40% of the total energy consumption in buildings. However, the operation of CACs is a complicated dynamic process with multiple subsystems and independent control loops. It is difficult to accurately regulate CACs to reach the required regulation services within the comfortable indoor temperature. To address this issue, this paper focuses on the quantitative assessment and two-layer coordinated controls of CACs to provide regulation services for the power system. Firstly, the thermal-electrical model of the CAC is established to describe the dynamic operation process of subsystems' characteristics. On this basis, a quantitative assessment method of CAC's regulation services is proposed by discretizing the thermal-electrical operation characteristics. Then, to aggregate multiple CACs to provide significant regulation capacities, an adaptive allocation method is proposed to satisfy the power system's regulation requirement based on different CACs' available regulation potential. Furthermore, an online distribution control method is developed to regulate each individual CAC's cooling capacity for guaranteeing the regulation accuracy and different occupants' comfortable temperatures. The effectiveness of the proposed models and methods is illustrated by numerical studies.

### 1. Introduction

The penetration rate of renewable energies is growing rapidly for reducing carbon emissions [1]. The fluctuating and intermittent

generation of non-dispatchable renewable energies results in more challenges of the system balance between generation-side and demand-side [2], which puts forward a higher requirement on the regulation service [3]. The regulation service is an essential auxiliary service in the

\* Corresponding authors at: Zhejiang University, NO.38 Zheda Road, Xihu District, Hangzhou 310027, China.

E-mail addresses: [xiekang@zju.edu.cn](mailto:xiekang@zju.edu.cn) (K. Xie), [hongxunhui@um.edu.mo](mailto:hongxunhui@um.edu.mo) (H. Hui), [yiding@zju.edu.cn](mailto:yiding@zju.edu.cn) (Y. Ding), [yhsong@um.edu.mo](mailto:yhsong@um.edu.mo) (Y. Song), [yechenjing@zju.edu.cn](mailto:yechenjing@zju.edu.cn) (C. Ye), [wdzheng@tju.edu.cn](mailto:wdzheng@tju.edu.cn) (W. Zheng), [yeshuiquan@runpaq.com](mailto:yeshuiquan@runpaq.com) (S. Ye).

power system for maintaining balance [4]. Traditional regulation services are mainly from generating units. However, the increasing renewable energies probably make the regulation services insufficient only by traditional generating units in the near future [5].

With advances in the information and communication technologies [6], demand-side flexible loads are paid more attention to provide regulation services for power systems, named as demand response (DR) [7]. Central air conditionings (CACs) are one of the most important flexible loads, because they are used in most commercial buildings [8]. Statistics indicate that CACs contribute to about 40% of the buildings' power consumption during peak load periods [9]. Therefore, CACs have huge potential to provide regulation services for power systems through adjusting their power consumption [10]. However, compared with the small residential split air conditioning for a single room (generally the rated power is  $1 \sim 2 \text{ kW}$ ) [11], one CAC can provide cooling capacity for hundreds of rooms, which makes the CAC's operation process become complicated [12]. The CAC consists of multiple subsystems and independent control loops with a variety of electrical equipment [13]. It is difficult to accurately regulate CACs to reach the required regulation services within the comfortable indoor temperature [14], which mainly involves the following twofold challenges:

*Regulation service assessment:* A challenging problem before implementing control on the CAC is quantitatively assessing the regulation service, because the available regulation capacity and time duration should be provided to the power system operator before each round of dispatch [15]. This topic has gained a few interests by researches. In [16], a regulation service assessment method is presented for the CAC by summing the compressor power that is turned off during the direct load control process. Reference [17] illustrates that the reduced power is proportional to the indoor area, thereby evaluating the regulation potential of the CAC. Quantitative evaluation method is established in [18] between the regulation capacity and the adjustment value of the indoor set temperature. However, these evaluation methods on CACs' regulation capacity are sketchy, because they calculate the regulation service by some indirect manners, such as the indoor area and the temperature reset [19]. To address this issue, this paper adopts a more direct manner by controlling the outlet set temperature of the CAC [20], because the power consumption of the CAC is determined by the difference between the outlet set temperature and the real-time outlet temperature [21]. The quantitative assessment method of the CAC's regulation service can be therefore obtained by discretizing the power control model. Some studies have focused on this power consumption adjustment method by experiment [22] and data fitting [23], while it has not been fully and systematically studied in the field of the quantitative assessment and the precise coordinated control of multiple CACs from the view of power systems.

*Precise control:* Each kind of regulation resources is generally dispatched by the power system operator. In order to guarantee the system's stable and secure operation, these regulation resources should provide the services within the required accuracy [24]. Compared with the regulation capacity from traditional generating units, one CAC's available regulation capacity is small. Generally, massive CACs need to be aggregated to provide regulation services, which further increases the difficulties of accurate control for each CAC. In [25], a two-way load control optimization approach is proposed for aggregated CACs by coordinating chiller units' operation states, i.e., ON or OFF. A real-time load control method is designed to accurately achieve the load shedding target by distributing the required regulation capacity between CACs [26]. A sequential dispatch method of the regulation capacity among different rooms is presented in [27] based on the set temperature to respond to the power system's regulation instructions [28]. The aforementioned studies mainly focus on the aggregate control, while each individual CAC is difficult to achieve the accurate regulation. In other words, some CACs may be regulated slightly, while some others are regulated significantly, and it may cause uncomfortable indoor temperature. In [29], a practical online controller is designed for the CAC in

the experiment to follow the secondary frequency regulation instruction from the power system. A feedback control method is proposed for the individual CAC to track the regulation requirement signal via its fan speed adjustment in [30]. An optimization mechanism of the individual CAC is proposed to respond to a variety of auxiliary service requirements based on predictive control of zone temperature in [31]. These researches do not pay attention to the allocation strategy of the regulation requirement for multiple CACs in power systems, especially in the condition of ensuring all the occupants' comfortable temperature [32].

To address the above challenges, the thermal-electrical model of the CAC is established to describe the dynamic characteristics from the perspective of power system. On this basis, a quantitative assessment method is presented to obtain the regulation capacity of the CAC by the outlet set temperature control. Power system operators can make regulation decisions based on the assessment results. Finally, a two-layer coordinated control method of CACs is proposed to provide regulation services for the power system. The control framework of CACs in this paper is shown in Fig. 1. The main contributions are summarized as follows:

- (1) Based on the dynamic operation model, a quantitative assessment method of CAC's regulation capacity is proposed by discretizing the thermal-electrical operation characteristics. Traditionally, the regulation capacity of small residential split air conditionings is evaluated by changing the room set temperature, which is not suitable for CACs with complicated operation process. The proposed method can precisely obtain the CAC's available regulation capacity by adjusting the outlet set temperature based on the CAC's internal model.
- (2) To aggregate multiple CACs to provide significant regulation capacities for the power system, an adaptive allocation method is proposed to regulate CACs' operating power based on different CACs' available regulation potential. Moreover, a fluctuation suppression control strategy is developed for CACs to guarantee the power system's regulation requirement under multiple uncertainties.
- (3) After receiving the allocated regulation service requirement, an online distribution control method is proposed to regulate each individual CAC's cooling capacity for guaranteeing the regulation accuracy and different occupants' comfortable temperatures. Moreover, a hysteretic control method is developed to introduce a dead band for reducing each room's repeated participation times during the regulation process.

The remaining of this paper is organized as follows. Section 2 develops the dynamic modeling and regulation capacity assessment method of the CAC for providing regulation services. Section 3 proposes an adaptive allocation method of the regulation service requirements among multiple CACs. Section 4 establishes an online distribution control method to regulate each individual CAC's cooling capacity. Case studies are carried out in Section 5, and Section 6 gives experiment analysis and application discussion of the control methods. Finally, Section 7 concludes this paper.

## 2. Modeling and regulation capacity assessment of the CAC for providing regulation services

In order to evaluate the regulation capacity of the CAC for providing regulation services, this section develops the thermodynamic model of the room firstly. Then, the thermal-electrical model of the CAC is established to integrate into the room's thermodynamic model. On this basis, a regulation capacity assessment method of the CAC is proposed by adjusting the outlet set temperature.

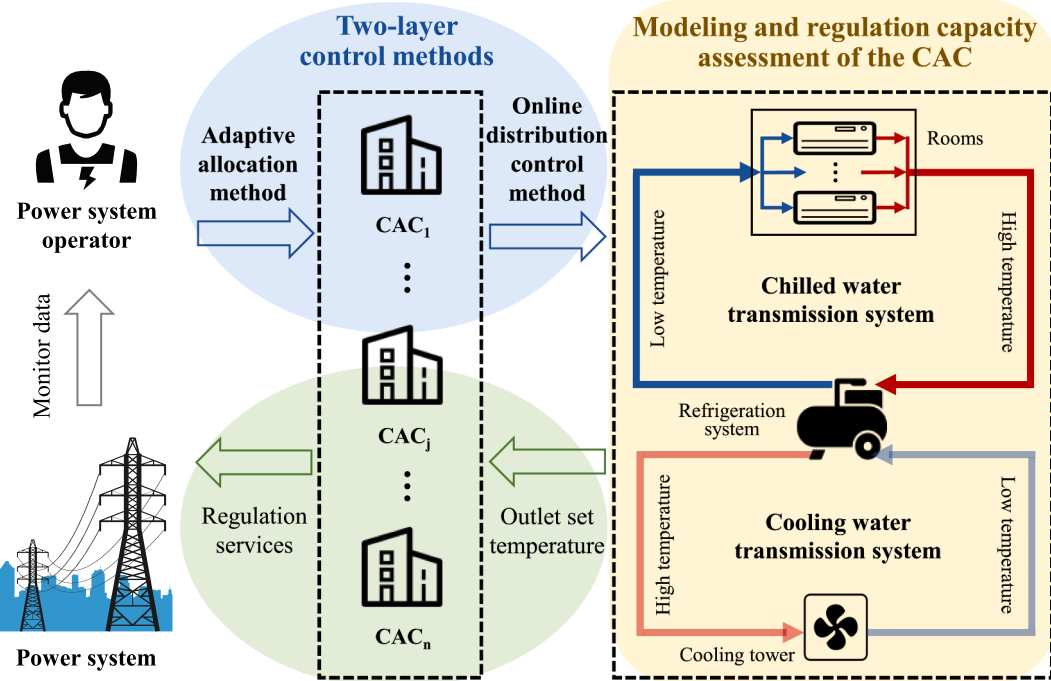


Fig. 1. The control framework of CACs.

## 2.1. Thermodynamic model of the room

Fig. 2 shows thermal dynamic process of the room, including the heating power  $Q_{ga}$  and the cooling capacity  $Q_{ch}^{fc}$  of the CAC [33]. The widely-used equivalent thermal parameter (ETP) model is adopted to describe thermodynamic process of the room [34]. Based on the ETP model, the thermal process of the indoor temperature can be expressed as:

$$C_a \frac{dT_{in}(t)}{dt} = -Q_{ch}^{fc}(t) + Q_{ga}^{sr}(t) + Q_{ga}^{hc}(t) + Q_{ga}^{in}(t) \quad (1)$$

$$Q_{ga}^{hc}(t) = \frac{T_o(t) - T_{in}(t)}{R_w} \quad (2)$$

$$Q_{ga}^{in}(t) = Q_{ga}^{ea}(t) + Q_{ga}^{ha}(t) + Q_{ga}^{ah}(t) \quad (3)$$

where  $C_a$  and  $R_w$  are the equivalent thermal capacity and the equivalent thermal resistance, respectively;  $T_o$  is the ambient temperature. The cooling capacity  $Q_{ch}^{fc}$  supplied to the room can be adjusted at the fan coil unit [35] to maintain indoor temperature at the setpoint [36], which can be described as:

$$Q_{ch}^{fc}(t) = \kappa_p^{fc}(T_{in}(t) - T_{in}^{set}) + \int_0^t \kappa_{in}^{fc}(T_{in}(t) - T_{in}^{set}) dt \quad (4)$$

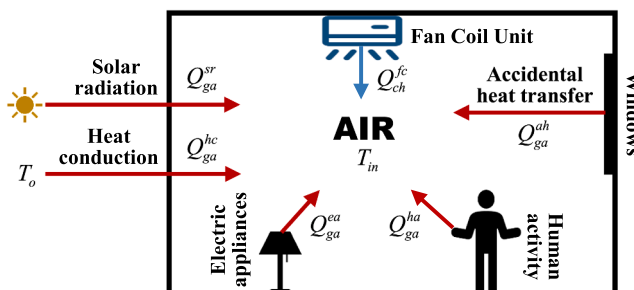


Fig. 2. The thermodynamic model of the room.

where  $\kappa_p^{fc}$  and  $\kappa_{in}^{fc}$  are the proportional factor and the integral factor for the feedback control of the room, respectively;  $T_{in}$  and  $T_{in}^{set}$  are the indoor real-time temperature and the indoor set temperature;  $Q_{ch}^{fc}$  should meet the power ramp rate constraint and the power constraint. The upper and lower limits are  $R_{min}^{fc}, R_{max}^{fc}, Q_{min}^{fc}$  and  $Q_{max}^{fc}$ , respectively.

## 2.2. Integrating the CAC electrical model into the room thermodynamic model

Fig. 3 shows a typical CAC system using water as the refrigerant to absorb thermal energy from rooms. The CAC is divided into three subsystems in this paper, including the chilled water transmission system, the refrigeration system and the cooling water transmission system [37]. The CAC model used in this paper comes from the *EnergyPlus* manual [38] and *Modelica Buildings Library* manual [39]. In the dynamic model, the subsystems' external characteristics are paid more attention to apply in the proposed assessment and control methods of following sections from perspective of power systems.

**Refrigeration system:** The refrigeration system is established according to the *ElectricEIR* model of the *Modelica Buildings Library* and *EnergyPlus*, which is described in more details in Appendix A. The refrigeration system is the cooling source of the chilled water. To maintain the outlet temperature at setpoint, the cooling capacity of the refrigeration system is determined by the difference between the outlet real-time temperature  $T_{ch}^o$  and the setpoint  $T_{set}^o$  [22,39], which can be expressed by:

$$Q_{ch}^{rs}(t) = \kappa_p^{rs}(T_{ch}^o(t) - T_{set}^o(t)) + \int_0^t \kappa_{in}^{rs}(T_{ch}^o(t) - T_{set}^o(t)) dt \quad (5)$$

where  $\kappa_p^{rs}$  and  $\kappa_{in}^{rs}$  are the proportional factor and the integral factor, respectively;  $T_{set}^o$  is the reference value of the outlet temperature. The cooling capacity  $Q_{ch}^{rs}$  should meet the power ramp rate constraint and the power constraint. The upper and lower limits are  $R_{min}^{rs}, R_{max}^{rs}, Q_{min}^{rs}$  and  $Q_{max}^{rs}$ , respectively. When the chilled water flows through the refrigeration system, the dynamic temperature rise can be expressed by [38]:

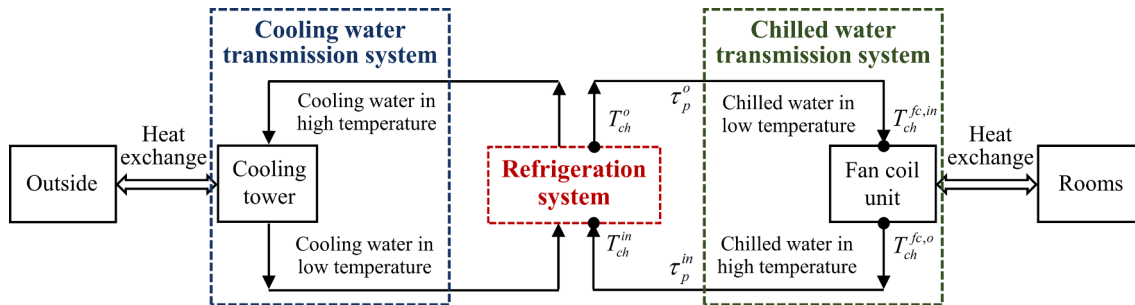


Fig. 3. The operation scheme of a typical CAC system.

$$Q_{ch}^{rs}(t) = c_w V_{con} \left( T_{ch}^{in}(t - \tau_p^{rs}) - T_{ch}^o(t) \right) \quad (6)$$

where  $c_w$  is the specific heat capacity of the chilled water;  $V_{con}$  is the mass flow rate of the chilled water;  $\tau_p^{rs}$  is the time duration when the chilled water flows through the refrigeration system. The relationship between the cooling capacity  $Q_{ch}^{rs}$  and electric power  $P_{ch}^{rs}$  can be expressed as [40]:

$$Q_{ch}^{rs}(t) = \kappa_{cop} P_{ch}^{rs}(t) \quad (7)$$

where  $\kappa_{cop}$  is the coefficient of performance (COP) of the CAC.

**Chilled water transmission system:** The chilled water transmission system can transfer cooling capacity from the refrigeration system to rooms. According to the *PlugFlowTransportDelay* model in the *Modelica Buildings Library*, there are two delay time during the chilled water transmission [41], including the outlet delay time  $\tau_p^o$  and the inlet delay

time  $\tau_p^{in}$ , which is shown in Fig. 3. The chilled water temperature will increase when it flows through rooms [39], which can be expressed by:

$$Q_{ch}^{fc}(t) = c_w V_{con} \left( T_{ch}^{fc,o}(t) - T_{ch}^{fc,in}(t - \tau_p^r) \right) \quad (8)$$

where  $\tau_p^r$  is the time duration when the chilled water flows through the room's fan coil unit. Eq. (8) model also comes from *MixingVolume* model in the *Modelica Buildings Library*, which is similar to Eq. (6).

**Cooling water transmission system:** The cooling water transmission system model refers to the *Condenser* model of the *ElectricEIR*. The cooling water can take away the heat generated by the refrigeration system for cooling. Considering this operation process is not the focus of this paper, it is expressed as a heat transfer process with delay  $\tau_p^c$ .

Therefore, the transfer function block diagram of the CAC operation model with the room's ETP model is developed using *Laplace Transform*,

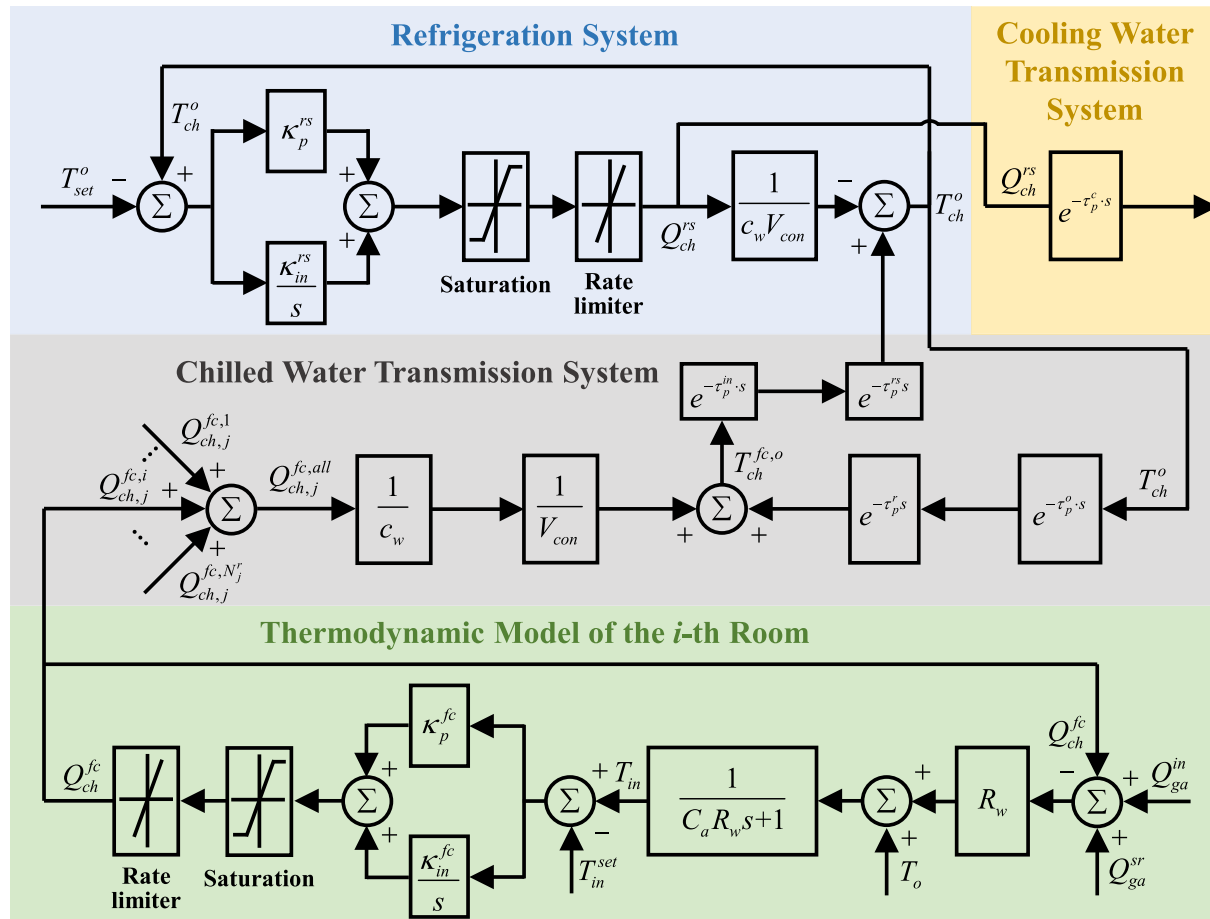


Fig. 4. The transfer function block diagram of the CAC.

which is shown in Fig. 4.

### 2.3. Quantitative assessment of the CAC's regulation capacity

The CAC can provide regulation services for the power system by changing its power consumption in the DR event. Before each round of dispatch, it is necessary for the power system operator to obtain the available regulation capacity of CACs. However, existing assessment methods (e.g., resetting the room set temperature) mainly focus on small residential split air conditionings, which are sketchy for CACs with complicated operation process. Therefore, a quantitative assessment method of CAC's regulation capacity is proposed by the direct manner based on the outlet temperature adjustment.

Based on the operation model, the CAC's power consumption can increase or decrease by adjusting the outlet set temperature, which is expressed by:

$$P_{ch}^{rs}(t) = \frac{\kappa_p^{rs}}{\kappa_{cop}} [T_{ch}^o(t) - (T_{set}^o + \Delta T_{set}^o)] + \frac{\kappa_{in}^{rs}}{\kappa_{cop}} \int_0^t [T_{ch}^o(t) - (T_{set}^o + \Delta T_{set}^o)] dt \quad (9)$$

where  $\Delta T_{set}^o$  is the increment of the outlet set temperature. The new outlet set temperature  $T_{set}^o + \Delta T_{set}^o$  needs to satisfy the constraint (i.e.,  $T_{set}^{min} \leq T_{set}^o + \Delta T_{set}^o \leq T_{set}^{max}$ ) to ensure the abnormal operation of the CAC.

When  $\Delta T_{set}^o < 0$ , the CAC can provide the downward reserve for the power system, which is equivalent to reducing output power of generators. Under these circumstances, the chilled water temperature becomes lower and hence it can supply enough cooling capacity to meet cooling demand of rooms. When  $\Delta T_{set}^o > 0$ , the CAC can provide the upward reserve for the power system, as generators increase the output power. In this case, the cooling capacity required by rooms cannot be satisfied, because the chilled water temperature is increased. Replace  $T_{set}^o + \Delta T_{set}^o$  with  $T_{set}^o$ , and the Eq. (9) can be discretized as:

$$P_{ch}^{rs}[t] = \frac{\kappa_p^{rs}}{\kappa_{cop}} (T_{ch}^o[t] - T_{set}^o[t]) + \frac{\kappa_{in}^{rs}}{\kappa_{cop}} \sum_{\tau=0}^t (T_{ch}^o[\tau] - T_{set}^o[\tau]) \quad (10)$$

Based on Eq. (10), the available regulation capacity  $\Delta P^a$  of the individual CAC at the next control duration can be obtained, which can be expressed by:

$$\Delta P^a[t+1] = \left[ (\kappa_p^{rs} + \kappa_{in}^{rs}) (T_{ch}^o[t+1] - T_{set}^{max}[t+1]) - \kappa_p^{rs} (T_{ch}^o[t] - T_{set}^o[t]) \right] / \kappa_{cop} \quad (11)$$

where  $T_{set}^{max}$  is the maximum outlet set temperature of the CAC. Therefore, the available regulation capacity of aggregate CACs can be expressed by:

$$\Delta P_{ag}^a[t+1] = \sum_{j=1}^{N_c^a} \Delta P_j^a[t+1] \quad (12)$$

where  $\Delta P_j^a$  is the available regulation capacity of aggregate CACs;  $\Delta P_j^a$  is the  $j$ -th CAC's available regulation capacity;  $N_c^a$  is the number of CACs that participate in the system regulation.

### 3. Adaptive allocation control method of the regulation requirement among CACs

In this section, an adaptive allocation method is proposed for power system operators to allocate the regulation service requirements among CACs based on their available regulation potential. That is to say, the power system operator will allocate the required regulation capacity  $P_s$  among CACs in the aggregation layer.

As shown in Fig. 5, the implemented duration  $t_{fd}$  of the DR event is monitored firstly. When  $t_{fd}$  is shorter than the regulation duration

requirement  $\tau_d$ , the control process of CACs will continue.

The system regulation capacity requirement is allocated according to the comprehensive regulation availability (CRA) of CACs. The CRA is defined as a row vector with two elements, including the temperature availability (TA) and the power availability (PA), which is:

$$CRA_j(t) = [TA_j(t), PA_j(t)] \quad (13)$$

where the subscript  $j$  refers to the  $j$ -th CAC. The  $TA_j$  and the  $PA_j$  can evaluate CAC's ability to provide regulation capacity for the power system in terms of the indoor temperature and the operating power, respectively. The  $TA_j$  and the  $PA_j$  of the  $j$ -th CAC can be expressed by:

$$TA_j(t) = \Phi(\Delta \bar{T}_j^{r,a}) / \sum_{j=1}^{N_c^a} \Phi(\Delta \bar{T}_j^{r,a}) \quad (14)$$

$$PA_j(t) = P_{ch}^{rs}(t) / \sum_{j=1}^{N_c^a} P_{ch}^{rs}(t) \quad (15)$$

where  $P_{ch}^{rs}$  is the operating power of the  $j$ -th CAC. Therefore, the regulation capacity requirement allocated to the  $j$ -th CAC can be expressed by:

$$P_s^j(t) = (\gamma_c TA_j(t) + \gamma_p PA_j(t)) P_s(t) \quad (16)$$

where  $\gamma_c$  and  $\gamma_p$  are the adaptive comfort and power weights, respectively and  $\gamma_c + \gamma_p = 1$ . Larger  $\gamma_c$  means that occupants' comfort is gotten more attention. When the allocated capacity  $P_s^j$  is larger than the available regulation capacity  $\Delta P_j^a$  of the  $j$ -th CAC,  $\gamma_c$  will be reduced until  $P_s^j \leq \Delta P_j^a$ . The average temperature deviation  $\Delta \bar{T}_j^{r,a}$  of the CAC can be expressed by:

$$\Delta \bar{T}_j^{r,a}(t) = \frac{\sum_{i=1}^{N_j^{r,a}} (T_{in,j}^i(t) - T_{in,j}^{set,i}(t))}{N_j^{r,a}} \quad (17)$$

where the superscript  $i$  and subscript  $j$  refer to the  $i$ -th room of  $j$ -th CAC;  $N_j^{r,a}$  is the number of rooms that can participate in the DR event for the  $j$ -th CAC;  $\Delta \bar{T}_j^{r,a}$  can describe the average temperature deviation of all rooms in the  $j$ -th CAC.

As shown in Fig. 6, based on the rooms' temperature deviation, the indoor temperature reserve function  $\Phi(\Delta \bar{T}_j^{r,a})$  is defined to describe the distance to the uncomfortable temperature boundary of rooms, which can be expressed by:

$$\Phi(\Delta \bar{T}_j^{r,a}) = \begin{cases} -\Delta \bar{T}_j^{r,a}(t) \frac{\Phi_{max}}{2\Delta T_{in}^{max}} + \frac{\Phi_{max}}{2}, & \text{if } P_s > 0 \& \Delta \bar{T}_j^{r,a} \in [\Delta T_{in}^{min}, \Delta T_{in}^{max}] \\ \Delta \bar{T}_j^{r,a}(t) \frac{\Phi_{max}}{2\Delta T_{in}^{max}} + \frac{\Phi_{max}}{2}, & \text{if } P_s < 0 \& \Delta \bar{T}_j^{r,a} \in [\Delta T_{in}^{min}, \Delta T_{in}^{max}] \\ 0, & \text{other} \end{cases} \quad (18)$$

where  $\Phi_{max}$  is the maximum value of  $\Phi(\Delta \bar{T}_j^{r,a})$ ;  $[\Delta T_{in}^{min}, \Delta T_{in}^{max}]$  is the comfortable indoor temperature deviation range;  $P_s$  is the regulation capacity requirement of the power system.  $P_s > 0$  means the CAC needs to reduce the operating power to provide the upward reserve for the power system. Conversely,  $P_s < 0$  means the CAC needs to provide the downward reserve for the power system. Taking  $P_s > 0$  as an example, the cooling capacity of the CAC is reduced in this case. The room temperature will increase. Therefore, the colder room has a longer duration to reach the uncomfortable boundary  $\Delta T_{in}^{max}$ , which means the room has a bigger indoor temperature reserve function value  $\Phi(\Delta \bar{T}_j^{r,a})$ .

Moreover, multiple uncertainties (e.g., the CAC's withdrawal from regulating or the change of the rooms' cooling demand) can impact the

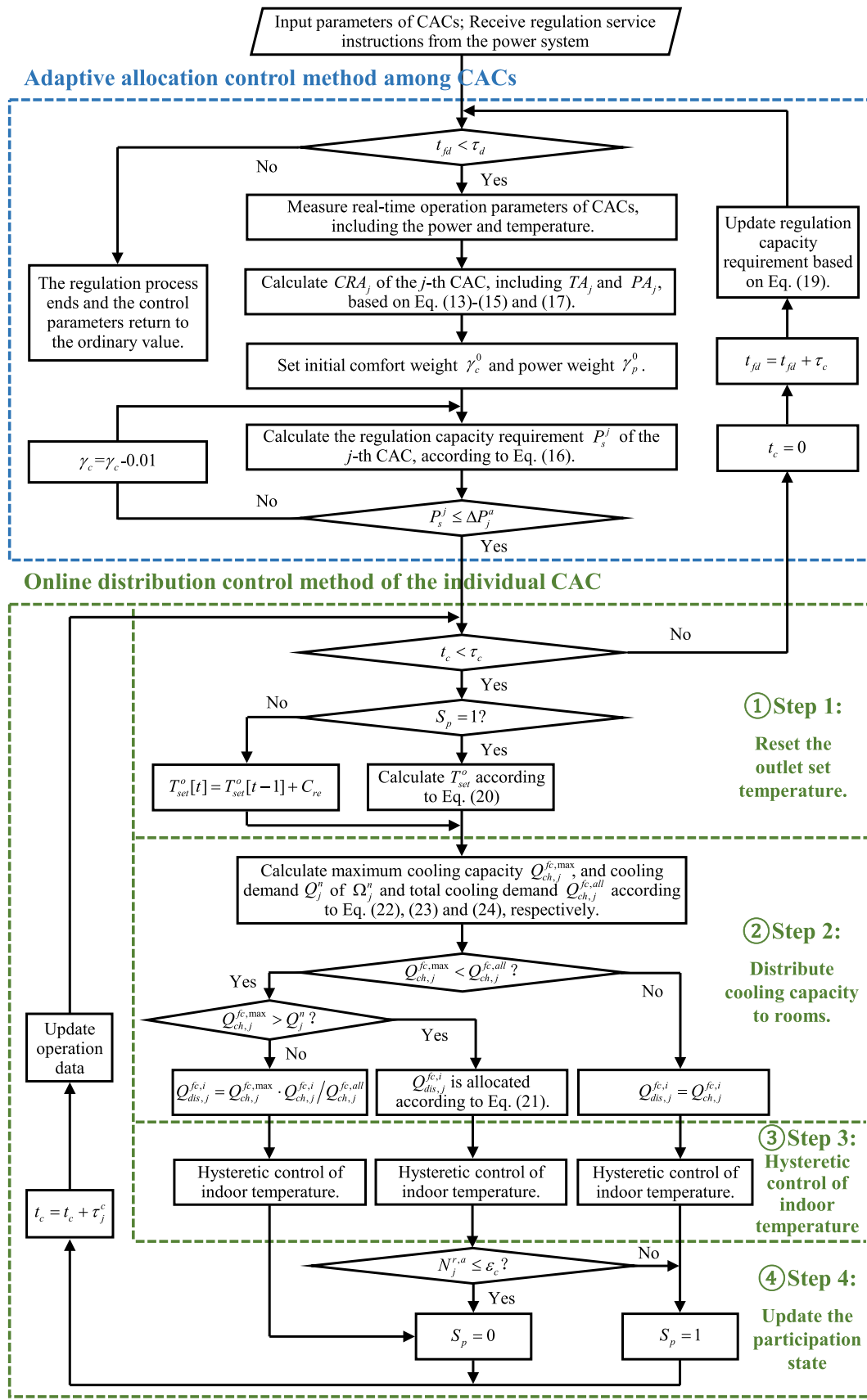


Fig. 5. The flow chart of CACs providing regulation services for the power system.

regulation accuracy. If the regulation capacity requirement still maintains constant, control errors will occur in the next regulation cycle. Therefore, a feedback control strategy is developed for the load fluctuation caused by these uncertainties, which can be expressed by:

$$P_s(t) = \kappa_p^s \left[ \sum_{j=1}^{N_c^a} P_{ch}^{rs}(t) - \left( \sum_{j=1}^{N_c^a} P_{ch}^{rs}(t_0) - P_s(t_0) \right) \right] + \kappa_{in}^s \int_0^t \left[ \sum_{j=1}^{N_c^a} P_{ch}^{rs}(t) - \left( \sum_{j=1}^{N_c^a} P_{ch}^{rs}(t_0) - P_s(t_0) \right) \right] dt \quad (19)$$

where  $P_s(t_0)$  and  $P_s$  are the initial regulation capacity requirement and the real-time updated regulation capacity requirement, respectively;  $P_{ch}^{rs}(t_0)$  is the operating power baseline and the stable operating power of the CAC before participating in regulation can be considered as  $P_{ch}^{rs}(t_0)$ ;  $\kappa_p^s$  and  $\kappa_{in}^s$  are the proportional factor and the integral factor, respectively. In this way, the regulation capacity requirement will be updated in each control cycle, and regulation errors caused by uncertainties will be eliminated.

#### 4. Online distribution control method for regulating individual CAC

$$Q_{dis,j}^{fc,i}(t) = \begin{cases} Q_{ch,j}^{fc,i}(t), & \text{if } Q_{ch,j}^{fc,max} \geq Q_{ch,j}^{fc,all} \\ Q_{ch,j}^{fc,i}(t), & \text{if } (Q_{ch,j}^{fc,all} > Q_{ch,j}^{fc,max} > Q_j^n) \cap (i \in \Omega_j^n) \\ Q_{ch,j}^{fc,i}(t) - (Q_{ch,j}^{fc,all}(t) - Q_{ch,j}^{fc,max}(t)) / N_j^{r,a}, & \text{if } (Q_{ch,j}^{fc,all} > Q_{ch,j}^{fc,max} > Q_j^n) \cap (i \in \Omega_j^p) \\ Q_{ch,j}^{fc,max}(t) \cdot Q_{ch,j}^{fc,i}(t) / Q_{ch,j}^{fc,all}(t), & \text{if } Q_{ch,j}^{fc,max} \leq Q_j^n \end{cases} \quad (21)$$

In this section, an online distribution control method is proposed for individual CAC to respond to the allocated regulation requirement under the premise of ensuring occupants' comfort. As shown in Fig. 5, to guarantee the regulation accuracy, power system operators will allocate the regulation capacity requirement to each CAC in every distribution period  $\tau_c$ . After receiving the regulation requirement, the four-step online distribution control method will be implemented for individual CAC.

##### Step 1: Reset the outlet set temperature.

The CAC can adjust its power consumption through resetting the outlet set temperature  $T_{set}^o$  based on the refrigerating system model. By discretizing and reversing Eq. (10), the specific control process can be expressed by:

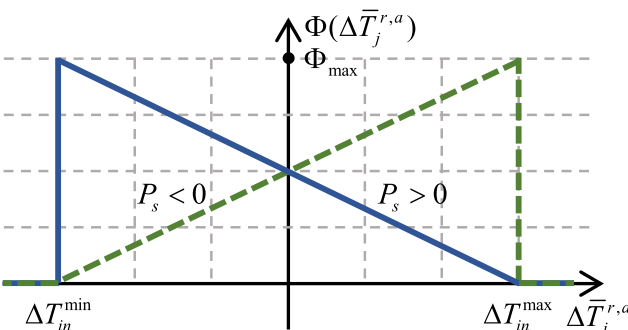


Fig. 6. The indoor temperature reserve function.

$$T_{set}^o[t] = \begin{cases} \frac{\kappa_{in}^{rs} T_{set}^o[t] + \kappa_p^{rs} T_{set}^o[t-1] + \kappa_{cop} (P_{ch}^{rs}[t-1] - P_{ch}^{rs}[t_0] + P_s^j[t-1])}{\kappa_p^{rs} + \kappa_{in}^{rs}}, & \text{if } S_p^j = 1 \\ T_{set}^o[t-1] + C_{re}, & \text{if } S_p^j = 0 \end{cases} \quad (20)$$

where  $P_s^j$  is the allocated regulation requirement for the  $j$ -th CAC. Symbol  $S_p^j$  is the participation state of the  $j$ -th CAC, where  $S_p^j = 1$  and  $S_p^j = 0$  mean the CAC continues and quits participating in system regulation, respectively. When the CAC quits regulating, the outlet set temperature is increased by an outlet recovery control constant  $C_{re}$  to provide enough cooling capacity for ensuring occupants' comfort.

##### Step 2: Distribute cooling capacity to rooms.

Rooms are divided into the participation group  $\Omega_j^p$  and the non-participation group  $\Omega_j^n$ , which will be updated in each distribution period. The participation group is the collection of rooms where their temperatures are within comfortable temperature ranges, while the non-participation group is the collection of rooms that exceed comfortable boundary.

During the system regulation process, the cooling capacity is not enough to meet cooling demand of rooms. To ensure the occupants' comfort, the cooling capacity supplied to the  $i$ -th room should be adjusted [32], which can be expressed by:

where  $Q_{ch,j}^{fc,i}$  is the cooling capacity demand of the  $i$ -th room based on Eq. (4). *i*) When the cooling demand can be satisfied (i.e.,  $Q_{ch,j}^{fc,max} \geq Q_{ch,j}^{fc,all}$ ), the cooling capacity supplied to each room is determined by its own cooling demand. *ii*) When the cooling capacity can satisfy the cooling demand of the non-participating rooms (i.e.,  $Q_{ch,j}^{fc,all} > Q_{ch,j}^{fc,max} > Q_j^n$ ), the cooling capacity will be supplied to ensure their comforts. *iii*) The remaining cooling capacity after the supply of non-participating rooms is allocated to the participating rooms. *iv*) When the cooling capacity of the chilled water cannot meet the cooling demand of the non-participating rooms (i.e.,  $Q_{ch,j}^{fc,max} \leq Q_j^n$ ), it will be allocated in proportion to the cooling demand of each room.  $Q_{ch,j}^{fc,max}$  is the CAC's maximum available cooling capacity, which can be expressed by:

$$Q_{ch,j}^{fc,max}(t) = c_w V_{con} (T_{ch}^{max}(t) - T_{ch}^{fc,in}(t - \tau_p^r)) \quad (22)$$

where  $T_{ch}^{max}$  is the maximum acceptable temperature of the chilled water to ensure heat exchange between the chilled water and rooms;  $V_{con}$  is the mass flow rate of the chilled water.  $Q_j^n$  is the total cooling demand of rooms that are in the non-participation group, which can be expressed by:

$$Q_j^n(t) = \sum_{i \in \Omega_j^n} Q_{ch,j}^{fc,i}(t) \quad (23)$$

The total cooling capacity demand required by all rooms can be expressed by:

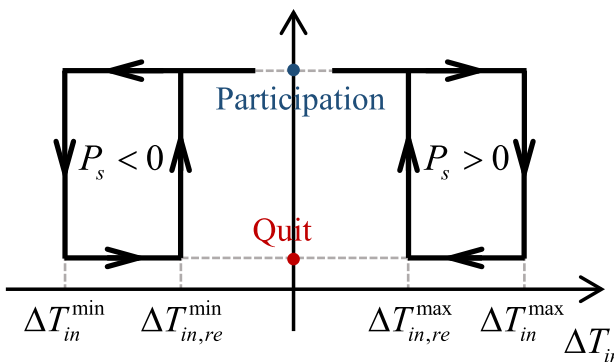


Fig. 7. The hysteretic control method of the indoor temperature.

$$Q_{ch,j}^{fc,all}(t) = \sum_{i=1}^{N_j^r} Q_{ch,j}^{fc,i}(t) \quad (24)$$

where  $N_j^r$  is the total room number of the  $j$ -th CAC.

The cooling capacity supplied to each room can be adjusted through resetting the indoor set temperature [42] based on Eq. (4), which can be expressed by:

$$T_{in,j}^{set,i}[t] = T_{in,j}^i[t] + \frac{\kappa_p^{fc} (T_{in,j}^i[t] - T_{in,j}^i[t-1]) + Q_{dis,j}^{fc,i}[t-1] - Q_{dis,j}^{fc,i}[t]}{\kappa_{in}^{fc}} \quad (25)$$

#### Step 3: Hysteretic control of indoor temperature.

A hysteretic control method is proposed to limit indoor temperature. The indoor temperature will be monitored in real time and limited within the dead-band comfortable temperature range as shown in Fig. 7. For example, when  $P_s > 0$ , the indoor temperature deviation will rise to  $\Delta T_{in}^{max}$  and then the room will quit regulating to recover the indoor temperature. Accordingly, when indoor temperature deviation returns to  $\Delta T_{in,re}^{max}$ , the room will participate in the regulation again. Therefore, the room's repeated participation times will decrease to reduce the impact on the occupant, compared with the comfortable temperature range without hysteretic control.

#### Step 4: Update the participation state.

In order to prevent the frequent adjustment of CAC's set parameters, the outlet set temperature  $T_{set}^o$  and the room's allocated cooling capacity  $Q_{dis,j}^{fc,i}$  will maintain constant in each CAC control period  $\tau_j^c$ . Meanwhile, the participation state  $S_p$  is updated and expressed by:

$$S_p(t) = \begin{cases} 1, & \text{if } (Q_{ch,j}^{fc,max} \geq Q_{ch,j}^{fc,all}) \cup (Q_{ch,j}^{fc,all} > Q_{ch,j}^{fc,max} > Q_j^n \cap N_j^{r,a} > \epsilon_c) \\ 0, & \text{if } (Q_{ch,j}^{fc,max} \leq Q_j^n) \cup (Q_{ch,j}^{fc,all} > Q_{ch,j}^{fc,max} > Q_j^n \cap N_j^{r,a} \leq \epsilon_c) \end{cases} \quad (26)$$

where  $\epsilon_c$  is the acceptable minimum number of rooms in the participation group  $O_j^p$ . When the cooling demand can be satisfied (i.e.,  $Q_{ch,j}^{fc,max} \geq Q_{ch,j}^{fc,all}$ ),  $S_p$  will be set to 1 and the CAC will continue to participate in the next round of the regulation process. When the cooling capacity cannot meet the cooling demand of the non-participating rooms (i.e.,

$Q_{ch,j}^{fc,max} \leq Q_j^n$ ),  $S_p$  will be set to 0 and the CAC will quit the regulation process. Moreover, when the cooling capacity can satisfy the cooling demand of the non-participating rooms (i.e.,  $Q_{ch,j}^{fc,all} > Q_{ch,j}^{fc,max} > Q_j^n$ ),  $S_p$  will be set to 1 if the number of the participating rooms is more than  $\epsilon_c$ . Otherwise,  $S_p$  will be set to 0 and the CAC will quit the regulation process.

## 5. Case study

### 5.1. Test system

The test system is built to illustrate the performance of the proposed control strategy, including 6 CACs with various operation parameters. These 6 CACs have large cooling capacity to serve shopping malls and theaters with large areas. The operation and control parameters of these CACs are shown in Table 1 [39].

It is assumed that every CAC has ten rooms with the random set temperature between 23°C and 26°C. The acceptable maximum indoor temperature deviation  $\Delta T_{in}^{max}$  is 1.5°C. The dead-band maximum indoor temperature deviation  $\Delta T_{in,re}^{max}$  is 1°C. Other room operation parameters of CACs are listed in Table 2 [43]. The operation parameters of the control system are shown in Table 3.

The regulation performance of the proposed control methods will be analyzed under different regulation capacity requirements  $P_s$ , control periods  $\tau_c$  and  $\tau_j^c$ , and multiple uncertainties. The time duration of the regulation process  $\tau_d$  is 30 min (i.e., from 500 s to 2300 s), and the ambient temperature is 32 °C. The models and methods are verified based on the tools *Modelica* and *Matlab*, with a computer i5-7400 CPU 3.00 GHz.

### 5.2. Results of different regulation capacities

The performance of the proposed control methods will be studied under the scenario of  $\tau_c = 50$  s,  $\tau_j^c = 5$  s, and  $\gamma_c^0 = 0.3$ , respectively. The regulation capacity requirements  $P_s$  are set to 0.2 MW, 0.3 MW, 0.4 MW, 0.5 MW and 0.6 MW, respectively. Fig. 8 shows the regulation results of CACs under different regulation capacity requirements. After small power fluctuations in the beginning, all regulation capacity requirements from power system operators are met by CACs through proposed control strategies. That is to say, CACs can accurately provide regulation services within 35% flexibility to meet different regulation requirements for 30 minutes.

Fig. 9 shows the set, outlet and inlet temperature curves of the CAC-1 and CAC-6 during the regulation process. It can be seen that all curves can maintain steady without huge fluctuations, and hence the control has little impact on CACs. In the beginning, the rise speed of the outlet set temperature becomes faster with the increase of the regulation capacity requirement. For example, Fig. 9 (c) has steeper outlet set temperature curve than Fig. 9 (a) at the beginning of the regulation when the regulation capacity increases from 0.2 MW to 0.6 MW. It means the operating power is changed more quickly for Fig. 9 (c). Therefore, different regulation capacity requirements can always be satisfied within a short time.

**Table 1**  
The operation and control parameters of CACs.

| Parameters | $\tau_p^o$ | $\tau_p^{in}$ | $V_{con}$ | $\tau_p^{rs}$ | $\tau_p^r$ | $\kappa_p^{rs}$ | $\kappa_{in}^{rs}$ | $R_{min}^{rs}$ | $R_{max}^{rs}$ | $Q_{min}^{rs}$ | $Q_{max}^{rs}$ |
|------------|------------|---------------|-----------|---------------|------------|-----------------|--------------------|----------------|----------------|----------------|----------------|
| Units      | s          | s             | kg/s      | s             | s          | kW/°C           | kW/(°C·s)          | kW/s           | kW/s           | kW             | kW             |
| CAC-1      | 50         | 50            | 150       | 5             | 5          | 800             | 5                  | -1050          | 1050           | 0              | 10,500         |
| CAC-2      | 45         | 45            | 115       | 5             | 5          | 800             | 3                  | -735           | 735            | 0              | 7350           |
| CAC-3      | 40         | 40            | 70        | 5             | 5          | 300             | 2                  | -420           | 420            | 0              | 4200           |
| CAC-4      | 32         | 32            | 42.5      | 3             | 3          | 200             | 1.2                | -210           | 210            | 0              | 2100           |
| CAC-5      | 27         | 27            | 22.5      | 3             | 3          | 120             | 0.7                | -105           | 105            | 0              | 1050           |
| CAC-6      | 22         | 22            | 12.5      | 3             | 3          | 100             | 0.5                | -52.5          | 52.5           | 0              | 525            |

**Table 2**

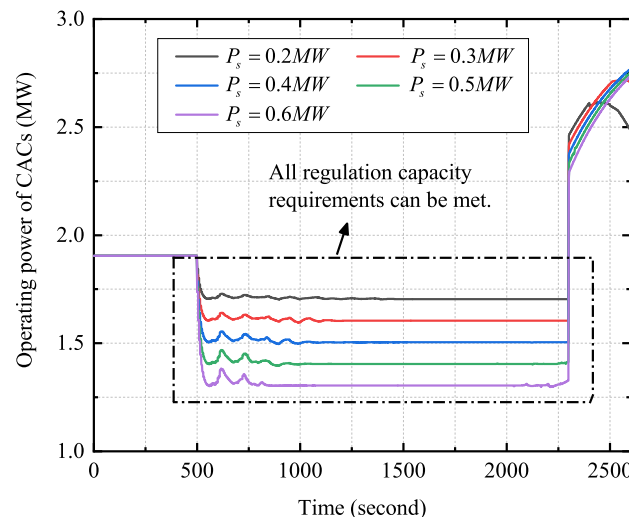
The operation parameters of rooms.

| Parameters | $C_a$      | $R_w$    | $Q_{ga}^{sr} + Q_{ga}^{in}$ | $\kappa_p^c$ | $\kappa_{in}^c$ | $R_{min}^c$ | $R_{max}^c$ | $Q_{min}^c$ | $Q_{max}^c$ |
|------------|------------|----------|-----------------------------|--------------|-----------------|-------------|-------------|-------------|-------------|
| Units      | J/°C       | °C/W     | kW                          | kW/°C        | kW/(°C·s)       | kW/s        | kW/s        | kW          | kW          |
| CAC-1 room | 1.00E + 08 | 2.68E-05 | 38                          | 400          | 0.12            | -100        | 100         | 0           | 1000        |
| CAC-2 room | 7.00E + 07 | 3.75E-05 | 26.6                        | 300          | 0.05            | -70         | 70          | 0           | 700         |
| CAC-3 room | 4.00E + 07 | 6.26E-05 | 15.2                        | 140          | 0.03            | -40         | 40          | 0           | 400         |
| CAC-4 room | 2.00E + 07 | 1.13E-04 | 7.6                         | 60           | 0.016           | -20         | 20          | 0           | 200         |
| CAC-5 room | 1.00E + 07 | 1.90E-04 | 3.8                         | 40           | 0.01            | -10         | 10          | 0           | 100         |
| CAC-6 room | 5.00E + 06 | 2.88E-04 | 1.9                         | 11           | 0.006           | -5          | 5           | 0           | 50          |

**Table 3**

The operation parameters of the control system.

| Names  | Parameters      | Values | Units           |
|--|-----------------|--------|-----------------|
| Proportional factor of fluctuation suppression control | $\kappa_p^s$    | 0.7    | —               |
| Integral factor of fluctuation suppression control     | $\kappa_{in}^s$ | 0.035  | s <sup>-1</sup> |
| Outlet recovery control constant                       | $C_{re}$        | -0.1   | °C              |
| Maximum acceptable temperature of chilled water        | $T_{ch}^{max}$  | 14     | °C              |
| Acceptable minimum number of rooms                     | $e_c$           | 5      | —               |

**Fig. 8.** The operating power of CACs under different regulation capacities.

Moreover, by comparing the CAC-1 and CAC-6 (e.g., Fig. 9 (a) and Fig. 9 (d)), the outlet set temperature curve of the CAC-6 is steeper than the CAC-1 in the beginning. It means that the power consumption of the CAC-6 is adjusted more quickly than the CAC-1, though the CAC-1 has larger operating power than the CAC-6. This is because the regulation capacity requirement is distributed according to both the power availability ( $PA_j$ ) and the temperature availability ( $TA_j$ ), instead of only the operating power. From the perspective of the temperature availability, the CAC-6 undertakes more regulation capacity percentage (the ratio of the allocated regulation capacity to the operating power) than CAC-1. In this manner, each room's comfortable temperature can be guaranteed better.

The comfort weight change under different regulation capacities is analyzed in Fig. 10. It can be seen that the comfort weight is difficult to maintain at the initial value with increase of the regulation capacity requirement. In particular, the initial comfort weight cannot completely be maintained under  $P_s = 0.6$  MW scenario during the whole regulation process, while it can be maintained all the time under  $P_s = 0.2$  MW scenario. Because a larger regulation capacity requirement needs to be achieved at a larger increase of the indoor temperature. To satisfy occupants' comfort, the proposed methods will decrease the regulation capacity from CACs with larger indoor temperature deviations.

### 5.3. Accuracy analysis under different control periods

The CACs' performance is analyzed under different control periods  $\tau_c$  and  $\tau_j^c$  when  $P_s = 0.4$  MW and  $\gamma_c^0 = 0.3$ , respectively. The control periods  $\tau_c$  and  $\tau_j^c$  are set to 10 s and 1 s, 50 s and 5 s, 100 s and 10 s, 200 s and 20 s, 300 s and 30 s, respectively.

The operating power of CACs is shown in Fig. 11 under different control periods. In the beginning, CACs do not meet the regulation requirements due to huge fluctuations, under the two scenarios of  $(\tau_c=300$  s,  $\tau_j^c=30$  s) and  $(\tau_c=200$  s,  $\tau_j^c=20$  s). Moreover, larger control period also brings control errors on the indoor temperature, as shown in Fig. 12. During the regulation process, the indoor temperature will rise beyond the upper limit of the comfort range under the two scenarios of  $(\tau_c=300$  s,  $\tau_j^c=30$  s) and  $(\tau_c=200$  s,  $\tau_j^c=20$  s). It is essential to select appropriate control periods to ensure the control accuracy of CACs (generally  $\tau_c$  is set less than 200 s and  $\tau_j^c$  is set less than 20 s).

Moreover, the implement of the comfortable indoor temperature range with a dead band (i.e., the hysteretic control method) can reduce each room's repeated participation times in regulation. As shown in Fig. 12, the room quits the regulation process when the indoor temperature exceeds the comfortable upper limit  $T_{in,6}^{set,1} + \Delta T_{in}^{max}$ . Then, when the indoor temperature decreases below  $T_{in,6}^{set,1} + \Delta T_{in,re}$ , the room will participate in the regulation process again. Without the hysteretic control method, the indoor temperature will fluctuate around the comfortable upper limit  $T_{in,6}^{set,1} + \Delta T_{in}^{max}$ . The proposed hysteretic control method can effectively avoid the repeated participation times and decrease the impact on the occupants.

### 5.4. Robustness analysis under multiple uncertainties

During the regulation process, there are some uncertainties. For example, the room cooling demand may change and the CAC may quit regulating. These two uncertain scenarios will result in load fluctuations and regulation errors. To deal with this problem, two control methods are compared here: (Method 1) the proposed fluctuation suppression control strategy, and (Method 2) the traditional load control method without fluctuation suppression. These two methods will be analyzed in two uncertain scenarios with  $P_s = 0.4$  MW,  $\tau_c=50$  s,  $\tau_j^c=5$  s and  $\gamma_c^0 = 0.3$ .

Scenario 1 is that the cooling demand of rooms is changed by  $\Delta Q_f$ , as shown in Fig. 13. The cooling demand change has three parts, including the ascending phase, the steady phase and the descending phase. These three phases represent the increase, stabilization and decrease of the room cooling demand. Fig. 14 shows the operating power of CACs under Method 1 and Method 2. Compared with Method 2, more than 95% of the load fluctuation amplitude can be completely eliminated to reduce the control errors under Method 1, which illustrates the effectiveness of the proposed fluctuation suppression control strategy.

Scenario 2 is caused by the CAC-3's withdrawal from regulating at 1400 s. As shown in Fig. 15, a large-value long-time power bounce occurs at the moment when the CAC-3 quits the regulation process under Method 2. When the proposed fluctuation suppression control strategy is implemented, only a short-time power shock appears. Subsequently, the

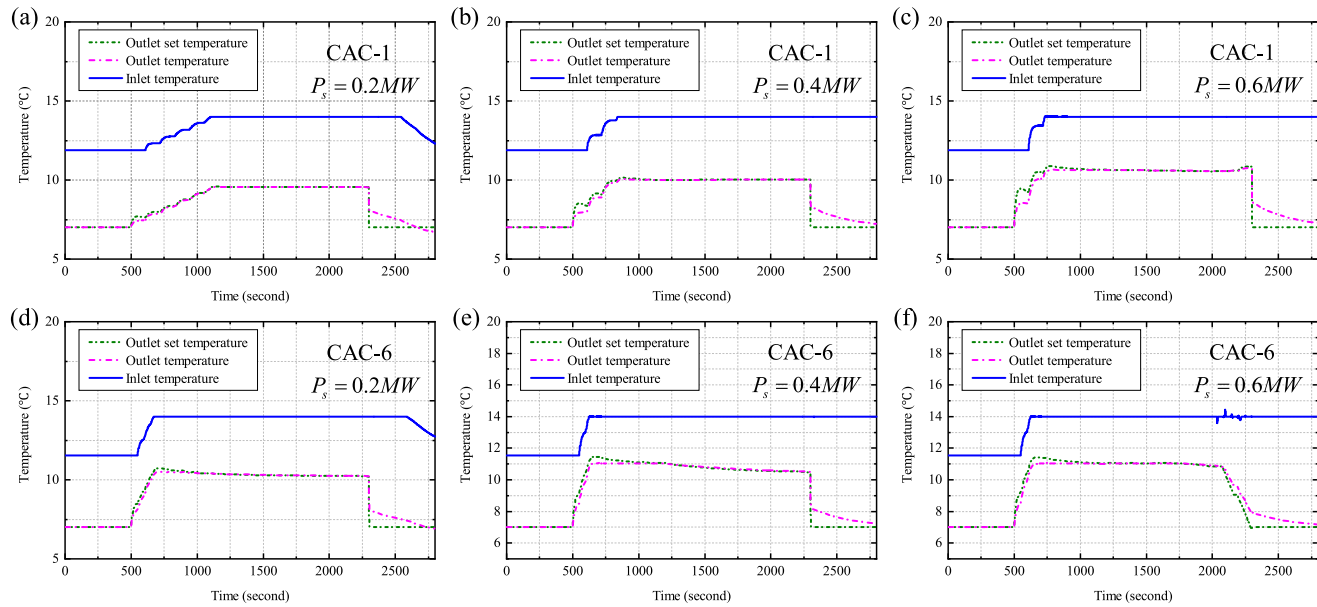


**Fig. 9.** The set, outlet and inlet temperature curves under different regulation capacity requirements when  $P_s$  is 0.2 MW, 0.4 MW and 0.6 MW: (a)-(c) are the temperature curves of the CAC-1; (d)-(f) are the temperature curves of the CAC-6.

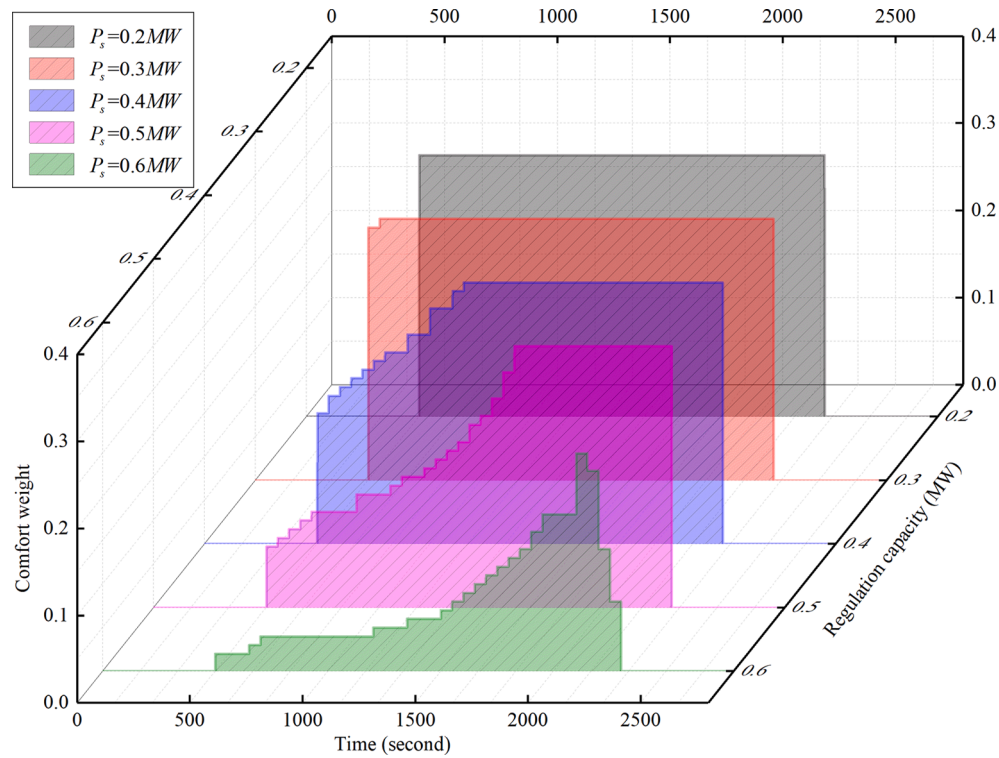


**Fig. 10.** The comfort weight change under different regulation capacities.

short-time power shock can be quickly eliminated to the required value and the steady power amplitude is less than 5% of that under Method 2.

## 6. Experiment analysis and application discussion of the control methods

To demonstrate the regulation effectiveness in practice, the proposed control methods are applied in realistic CAC system data through *EnergyPlus*. Moreover, discussions are made to analyze application of the proposed control methods in practice, including the system parameters,

measurement parameters and control parameters. On this basis, some experiments are conducted under inaccurate parameters to verify the effectiveness of the proposed methods.

### 6.1. Experiment analysis of the control methods in practice

#### (1) Test system

The test system is built based on the file *ElectricChiller* of the *EnergyPlus*. The *ElectricChiller* is a realistic CAC system, which considers the

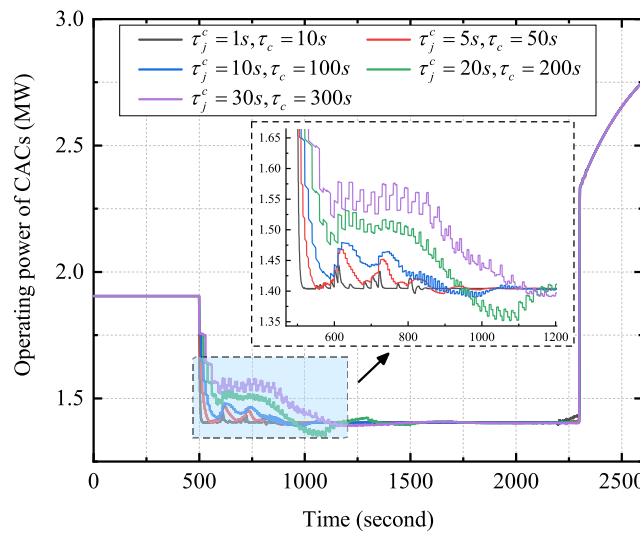


**Fig. 11.** The operating power of CACs under different control periods.

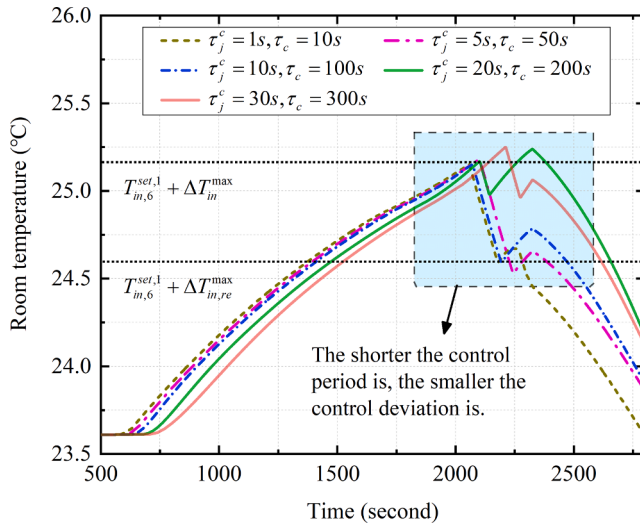


**Fig. 12.** The room temperature of CAC-6 under different control periods.

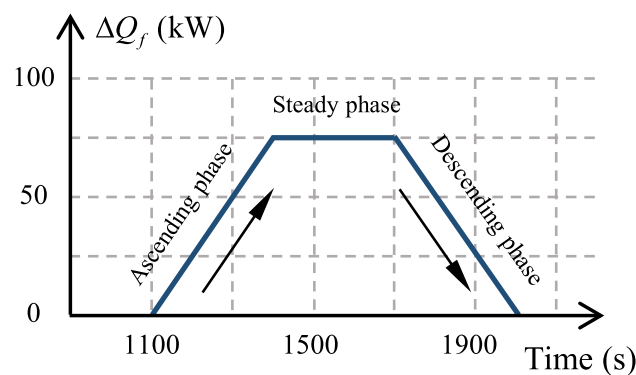


**Fig. 13.** The change of the room cooling demand.

complicated heat transfer process and hydraulic process. The building has five rooms with the height of 3 m and in the size of 100 m<sup>2</sup>, 100 m<sup>2</sup>, 40 m<sup>2</sup>, 40 m<sup>2</sup> and 180 m<sup>2</sup>, respectively. Each room has time-varying heat gains from people, lights and other electric equipment. Table 4 shows the rated power of indoor loads.

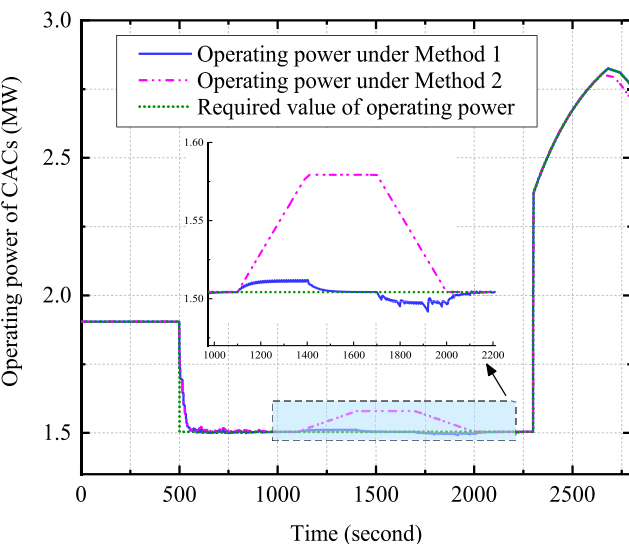


**Fig. 14.** The operating power of CACs when the room cooling demand changes.

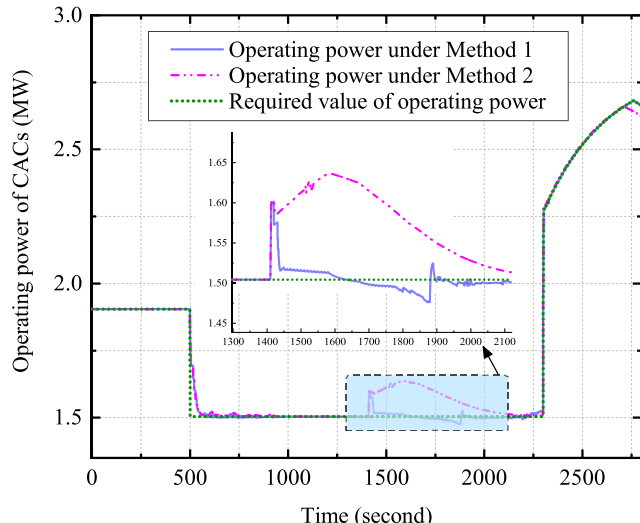


**Fig. 15.** The operating power of CACs when the CAC-3 quits regulating at 1400 s.

**Table 4**  
The rated power of indoor loads.

| Names            | Units   | Room-1 | Room-2 | Room-3 | Room-4 | Room-5 |
|------------------|---------|--------|--------|--------|--------|--------|
| Number of people | persons | 5      | 5      | 3      | 3      | 9      |
| Lights           | W       | 1600   | 1600   | 700    | 700    | 3000   |
| Other equipment  | W       | 1100   | 1100   | 400    | 400    | 2000   |

The CAC system with a water-cooled electric chiller provides the cooling capacity for the building. The chiller is built based on the widely-used *ElectricEIR* in *EnergyPlus*, which considers the complex time-varying thermal transfer process. The main parameters of the CAC system are shown in Table 5.

In order to accurately calculate the room thermal response, a detailed building structure is considered and built, including walls, windows, doors and sunlight. The walls are shingled over plywood, R11 insulation, and gypsum board. The windows on all the 4 facades are 3 mm

**Table 5**  
Main parameters of the CAC chiller.

| Names  | Units             | Values  | Names   | Units | Values |
|--|-------------------|---------|---|-------|--------|
| Nominal capacity                             | W                 | 100,000 | The 1st coefficient for power ratio curve     | -     | 1.908  |
| Nominal COP                                  | W/W               | 3.75    | The 2nd coefficient for power ratio curve     | -     | -1.205 |
| Design water flow rate                       | m <sup>3</sup> /s | 0.0011  | The 3rd coefficient for power ratio curve     | -     | 0.263  |
| The 1st coefficient for capacity ratio curve | -                 | 0.945   | The 1st coefficient for full load ratio curve | -     | 0.033  |
| The 2nd coefficient for capacity ratio curve | -                 | -0.057  | The 2nd coefficient for full load ratio curve | -     | 0.685  |
| The 3rd coefficient for capacity ratio curve | -                 | -0.0019 | The 3rd coefficient for full load ratio curve | -     | 0.282  |

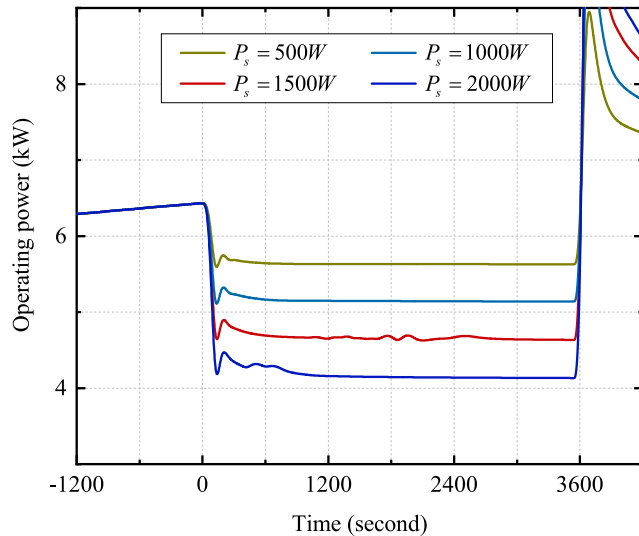


**Fig. 16.** The operating power of the CAC under different regulation capacity requirements.

glass. The window to wall ratio is approximately 0.29. The south and north facades have glass doors with overhangs. The roof is a gravel built-up roof with R3 mineral board insulation and plywood sheathing. The building is oriented 30 degrees east of north.

The ambient temperature is derived from the realistic summer temperature in Washington of the file “USA\_VA\_Sterling-Washington.Dulles.Intl.AP.724030\_TMY3”. The above models and the proposed control methods are verified in *EnergyPlus* with the time step of 1 minute using a computer i5-7400 CPU 3.00 GHz.

## (2) Regulation results

**Fig. 16** shows the regulation results in four cases with different regulation capacities, including 500 W, 1000 W, 1500 W, and 2000 W. After receiving the regulation instruction, the CAC can reach the required regulation capacities in about 1 min. Then the CAC can maintain the operating power for an hour to continuously provide regulation services for the power system. Therefore, the proposed control methods can work well for CAC systems considering complex thermal and hydraulic processes.

**Fig. 17** gives the inlet and outlet temperatures of the CAC system during the regulation process. The experimental results on the realistic

CAC can prove: (i) the proposed control method can keep the chilled water temperature stable, which avoids fluctuations and reduces the impact on the CAC system; (ii) the rise speed of the chilled water temperature can be increased in a higher regulation capacity scenario to improve the CAC's power regulation speed.

**Fig. 18** shows the room temperature curves under different regulation capacity scenarios with the set temperature 25°C. It can be seen that the room temperatures can always be limited within the acceptable range [-1.5°C, 1.5°C] to guarantee occupants' comforts. Moreover, another scenario  $P_s = 2500\text{W}$  is supplemented to illustrate the hysteretic temperature control method. In **Fig. 18(d)**, Room-3 uses the hysteretic temperature control method, while other rooms are controlled without the hysteretic process. It can be seen that the Room-3 can withdraw the regulation process when the indoor temperature reaches the upper limit. The Room-3 will participate in the control process again, when the indoor temperature is reduced to be lower 0.5°C than the upper limit. Therefore, the proposed hysteretic temperature control method can avoid the room to repeatedly participate in the regulation service and decrease the impact on occupants.

## 6.2. Application discussion of the control methods in practice

### (1) System parameters

The system parameters for the proposed control strategy are shown in **Table 6**.

The system parameters mainly include three types:

Type 1: Parameters determined by the power system operator.

These parameters are sent to CACs by the power system operator according to the real-time power system operation requirement, including the regulation capacity  $P_s$ , regulation duration  $t_d$ , and the CAC control period  $t_p^c$ .

Type 2: Parameters determined by the CAC's product manual.

These parameters are obtained according to the CAC's product manual and its setting values, including the proportional factors  $\kappa_p^{rs}$  and  $\kappa_p^{fc}$ , the integral factors  $\kappa_{in}^{rs}$  and  $\kappa_{in}^{fc}$ , and the maximum acceptable temperature of the chilled water  $T_{ch}^{max}$ .

Type 3: Parameters determined by the proposed control method.

These parameters are determined by the CAC users according to their comfort preferences, including the upper and lower limits of the room temperature deviation [ $\Delta T_{in}^{min}, \Delta T_{in}^{max}$ ], the maximum and minimum indoor temperature deviations for hysteretic control [ $\Delta T_{in,re}^{min}, \Delta T_{in,re}^{max}$ ], the maximum value of the indoor temperature reserve function  $\Phi_{max}$ , and the recovery control constant of the outlet  $C_{re}$ .

Typically,  $\Delta T_{in,re}^{min} = \Delta T_{in}^{min} + 0.5$ ,  $\Delta T_{in,re}^{max} = \Delta T_{in}^{max} - 0.5$  and  $C_{re} = -0.1$ . The parameter  $\Phi_{max}$  is the maximum value of the indoor temperature reserve function  $\Phi(\bar{T}_j^{r,a})$ , which describes the distance to the uncomfortable temperature boundary of rooms. In this paper, the parameter  $\Phi_{max}$  is set as 1.5°C.

### (2) Measurement parameters

The measurement parameters for the proposed control strategy are shown in **Table 7**.

The measurement parameters mainly include two types:

Type 1: Measurement parameters provided by the building automation system.

The building automation system (BAS) has been widely installed in buildings to monitor the operation states of the CAC. Some parameters can be obtained directly by the BAS, including the indoor temperature  $T_{in,j}^i$ , the outlet temperature  $T_{ch}^o$ , the CAC operating power  $P_{ch}^s$  and the mass flow rate of the chilled water  $V_{con}$ .

Type 2: Measurement parameters that can be calculated using known data.

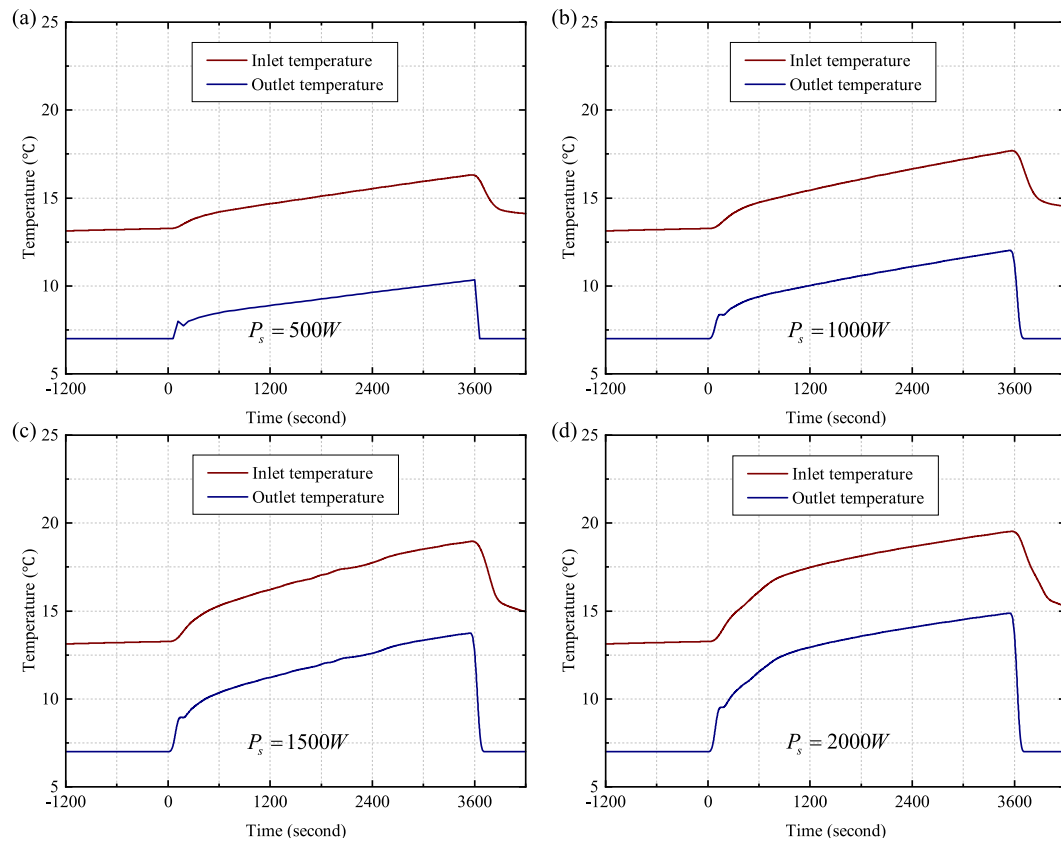


**Fig. 17.** The inlet and outlet temperatures under different regulation capacity requirements: (a) $P_s = 500W$ ; (b) $P_s = 1000W$ ; (c) $P_s = 1500W$ ; (d) $P_s = 2000W$ .

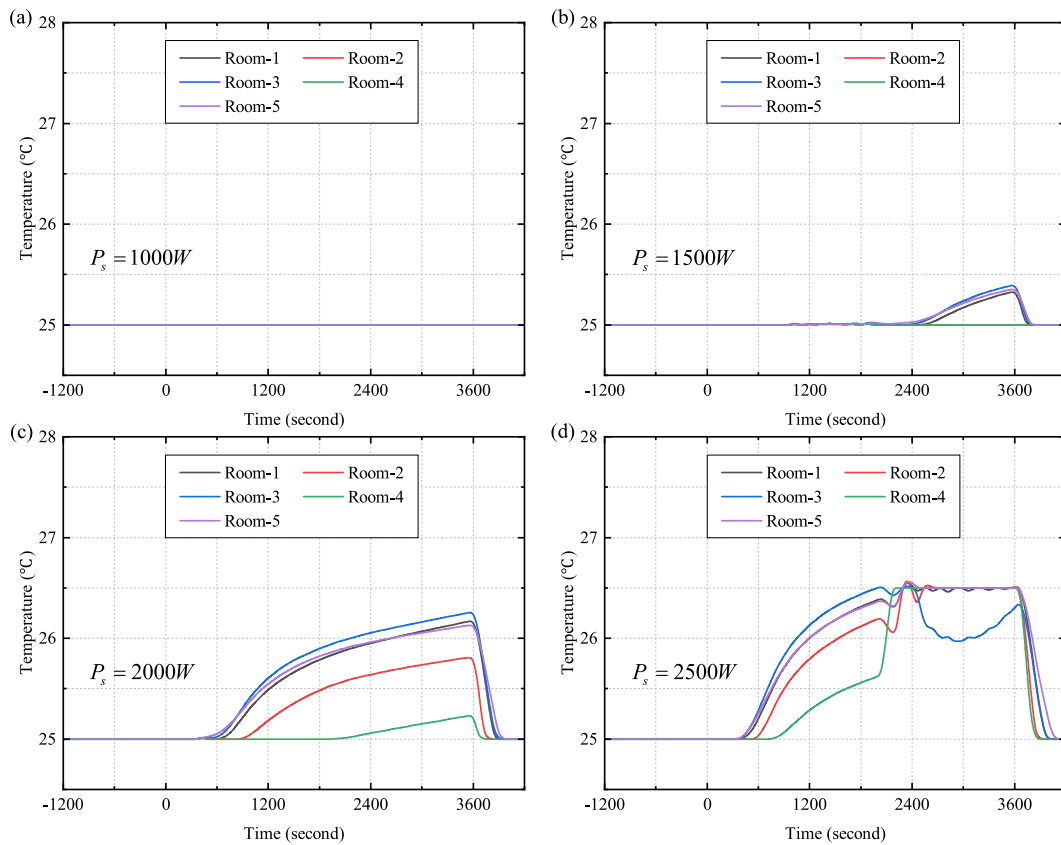


**Fig. 18.** The room temperature curves under different regulation capacity requirements: (a) $P_s = 1000W$ ; (b) $P_s = 1500W$ ; (c) $P_s = 2000W$ ; (d) $P_s = 2500W$ .

**Table 6**  
System parameters used for the proposed control strategy.

| Names   | Symbols                   | Units     | Types  |
|---|---------------------------|-----------|--|
| Regulation capacity requirement                             | $P_s$                     | kW        |  |
| Regulation duration requirement                             | $\tau_d$                  | s         | Type 1: Parameters determined by the power system operator   |
| CAC control period  | $\tau_j^c$                | s         |  |
| Proportional factor of the power control                    | $k_p^s$                   | kW/°C     |  |
| Integral factor of the power control                        | $k_{in}^s$                | kW/(°C·s) |  |
| Proportional factor of the room cooling capacity            | $k_p^{fc}$                | kW/°C     | Type 2: Parameters determined by the CAC's product manual    |
| Integral factor of the room cooling capacity                | $k_{in}^{fc}$             | kW/(°C·s) |  |
| Maximum acceptable temperature of the chilled water         | $T_{ch}^{\max}$           | °C        |  |
| Upper limit of the indoor temperature deviation             | $\Delta T_{in}^{\max}$    | °C        |  |
| Lower limit of the indoor temperature deviation             | $\Delta T_{in}^{\min}$    | °C        |  |
| Maximum indoor temperature deviation for hysteretic control | $\Delta T_{in,re}^{\max}$ | °C        |  |
| Minimum indoor temperature deviation for hysteretic control | $\Delta T_{in,re}^{\min}$ | °C        | Type 3: Parameters determined by the proposed control method |
| Maximum value of the indoor temperature reserve function    | $\Phi_{\max}$             | °C        |  |
| Recovery control constant of the outlet                     | $C_{re}$                  | °C        |  |

**Table 7**  
Measurement parameters used for the proposed control strategy.

| Names  | Symbols           | Units | Types   |
|--|-------------------|-------|---|
| Real-time indoor temperature                                   | $T_{in,j}$        | °C    |   |
| Real-time outlet temperature                                   | $T_{ch}$          | °C    | Type 1: Measurement parameters provided by the building automation system |
| CAC operating power  | $P_{ch}^s$        | kW    |   |
| Mass flow rate of the chilled water                            | $V_{con}$         | kg/s  |   |
| Cooling capacity supplied to a room                            | $Q_{ch,j}^{fc,i}$ | kW    | Type 2: Measurement parameters that can be calculated using known data    |
| Duration of the chilled water through the room's fan coil unit | $\tau_p^r$        | s     |   |

**Table 8**  
Control parameters used for the proposed control strategy.

| Names  | Symbols            | Units |
|--|--------------------|-------|
| Regulation instruction of the outlet set temperature | $T_{set}^o$        | °C    |
| Regulation instruction of the indoor set temperature | $T_{in,j}^{set,i}$ | °C    |

This type of system parameters cannot be used directly, while they can be calculated from known measurement data, including the CAC cooling capacity  $Q_{ch,j}^{fc,i}$  and the duration of the chilled water through the room's fan coil unit  $\tau_p^r$ . The CAC cooling capacity can be calculated by Eq. (4) and all used parameters are available to calculate the CAC cooling capacity  $Q_{ch,j}^{fc,i}$ . The duration  $\tau_p^r$  can be calculated by the pipe length of the room's fan coil unit and the flow rate of the chilled water.

### (3) Control parameters

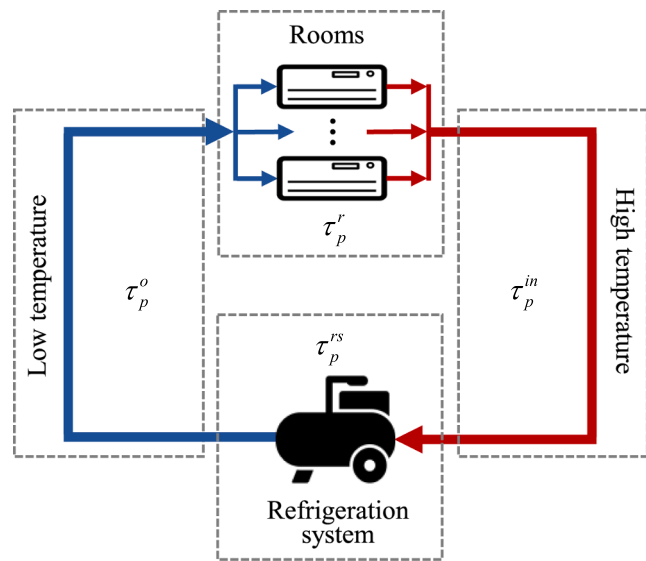


**Fig. 19.** The time delay parameters of a typical CAC system.

The control parameters for the proposed control strategy are shown in Table 8.

In the proposed control strategy, two control parameters are required for the corresponding controllers, i.e., the regulation instructions for the outlet set temperature  $T_{set}^o$  and the indoor set temperature  $T_{in,j}^{set,i}$ . The instruction for the outlet set temperature can change the CAC's operating power. The instruction for the room set temperature can change the cooling demand. These two control parameters can be set through the BAS.

### (4) Performance analysis under inaccurate parameters of practical systems

The above parameters (i.e., system parameters, measurement parameters, and control parameters) can be determined in practical systems. However, some parameters may be captured inaccurately, such as the time parameters  $\tau_p^o$ ,  $\tau_p^in$ ,  $\tau_p^rs$ , and  $\tau_p^r$ . More experiments are therefore conducted under these inaccurate parameters to verify the effectiveness of the proposed method.

Parameters  $\tau_p^o$ ,  $\tau_p^in$ ,  $\tau_p^rs$ , and  $\tau_p^r$  are the time delays due to the flow of chilled water in the pipe. Their values are the ratios of the corresponding pipe lengths to the flow rates of the chilled water, as shown in Fig. 19. The outlet delay  $\tau_p^o$  is the period of the chilled water flow from the refrigeration system to the room's fan coil unit. The inlet delay time  $\tau_p^in$  is the period of the chilled water flow from the room's fan coil unit to the refrigeration system. The time duration  $\tau_p^rs$  is the period of the chilled water flow through the refrigeration system. The time duration  $\tau_p^r$  is the period of the chilled water flow through the room's fan coil unit. It is assumed that these four delays are detected inaccurately, whose errors are denoted as  $\epsilon_p^o$ ,  $\epsilon_p^in$ ,  $\epsilon_p^rs$  and  $\epsilon_p^r$ , respectively.

Fig. 20 shows the CAC operating power under different delay errors from -20% to 20%. It can be seen that the curves in each case almost completely overlap, which means the inaccurate delay parameters have little impacts on the control results. Therefore, the regulation deviation caused by the delay errors can be ignored.

## 7. Conclusions

In order to track the shortage of the regulation services, this paper proposes the quantitative assessment and precise control methods of CACs to provide regulation services for the power system. First, the

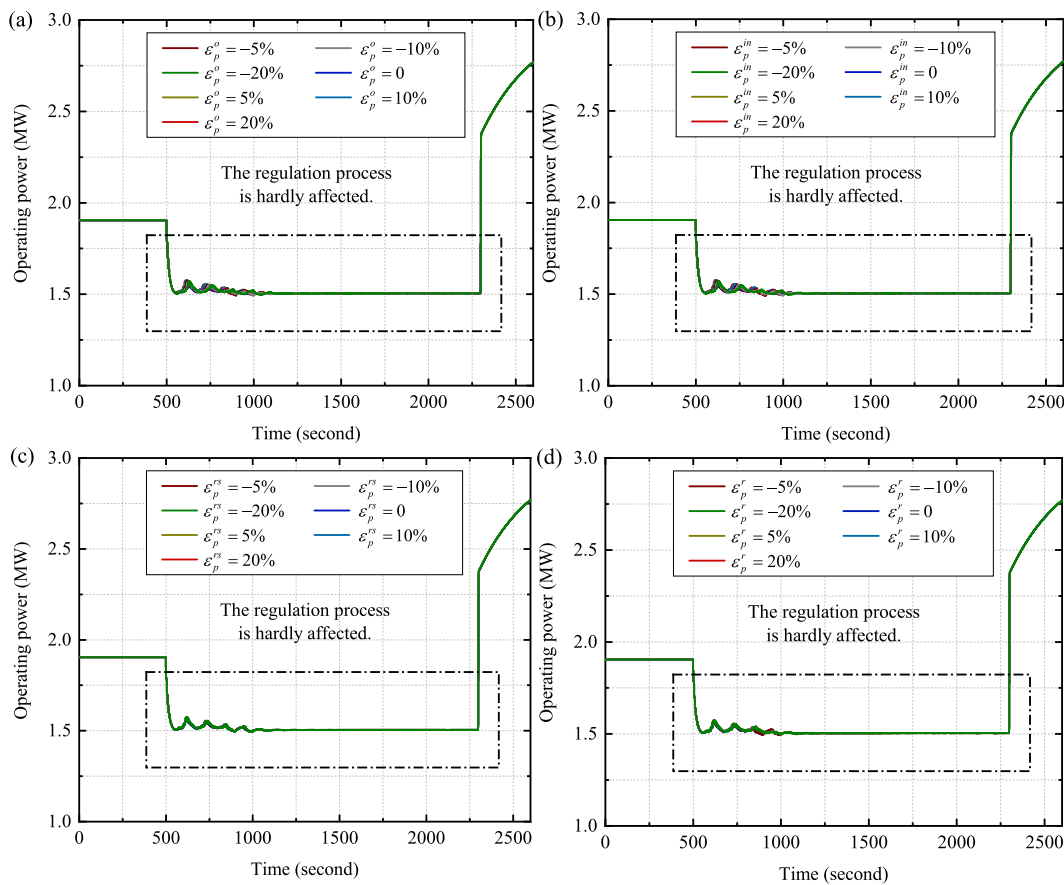


**Fig. 20.** The CAC operating power under inaccurate delay time: (a) under the outlet delay time error; (b) under the inlet delay time error; (c) under the duration error through the refrigeration system; (d) under the duration error through the room's fan coil unit.

thermal-electrical model of the CAC is established to describe the dynamic operation process, including the chilled water transmission system, the refrigeration system and the cooling water transmission system. Then, by discretizing the thermal-electrical operation process, a quantitative assessment method is developed for evaluating CAC's regulation capacity. In this manner, the CAC's power consumption can be precisely controlled to participate in the DR event by adjusting the outlet set temperature. On this basis, an adaptive allocation method is proposed to aggregate multiple CACs to provide significant regulation capacities for the power system based on different CACs' available regulation potential. A feedback control strategy is developed for eliminating load fluctuations caused by multiple uncertainties, such as the room cooling demand change and the CAC's withdrawal from regulating. Finally, an online distribution control method is proposed to regulate each individual CAC's cooling capacity for guaranteeing the regulation accuracy and different occupants' comfortable temperatures.

The regulation performance of the proposed modeling and control strategy is illustrated under different control parameters by several cases, including regulation capacity requirements, control periods and multiple uncertainties. The results show that CACs can accurately provide regulation services within 35% flexibility to meet different regulation requirements for 30 minutes. Meanwhile, the proposed control methods can limit the indoor temperature deviations within occupants' comfortable ranges about [-1.5°C, 1.5°C]. The operating power bounce

caused by uncertainties can also be significantly reduced by about 95% during the regulation process.

#### CRediT authorship contribution statement

**Kang Xie:** Methodology, Software, Validation, Formal analysis, Writing – original draft, Writing – review & editing. **Hongxun Hui:** Conceptualization, Formal analysis, Writing – review & editing. **Yi Ding:** Conceptualization, Methodology, Writing – review & editing, Project administration. **Yonghua Song:** Conceptualization, Supervision, Project administration. **Chengjin Ye:** Resources, Data curation, Validation. **Wandong Zheng:** Validation, Writing – review & editing. **Shuiquan Ye:** Investigation, Validation.

#### Declaration of Competing Interest

The authors declare that they have no known competing financial interests or personal relationships that could have appeared to influence the work reported in this paper.

#### Acknowledgements

This work is supported by the National Science Foundation for Distinguished Young Scholars of China under Grant 52125702.

#### Appendix A

The refrigeration system is established according to the *ElectricEIR* model of the *Modelica Buildings Library* and *EnergyPlus*. The specific modeling process is as follows.

*Cooling capacity model in Eq. (5):* The cooling capacity adjustment model of the refrigeration system refers to *PartialElectric* model of the *ElectricEIR*. In this model, the cooling capacity provided by the refrigeration system to the chilled water is proportional to the difference between the outlet temperature and the set temperature. On this basis, an integral part is also added in this paper to represent the slow heat transfer process, as shown in Eq. (5).

*Chilled water model in Eq. (6):* The chilled water model comes from the *MixingVolume* model of the *ElectricEIR*. In this model, the internal energy for the chilled water is adjusted by the cooling capacity of the refrigeration system, which is expressed as:

$$\frac{dU}{dt} = Hb_{flow} + Q_{flow} \quad (27)$$

where  $U$  is the internal energy for the chilled water;  $Hb_{flow}$  and  $Q_{flow}$  are the enthalpy of the chilled water and the cooling capacity of the refrigeration system, respectively. Based on CAC variables in this paper, the model in Eq. (27) can be reformulated as the Eq. (6).

## References

- [1] Cheng Y, Zhang N, Kirschen DS, Huang W, Kang C. Planning multiple energy systems for low-carbon districts with high penetration of renewable energy: An empirical study in China. *Appl Energy* 2020;261:114390. <https://doi.org/10.1016/j.apenergy.2019.114390>.
- [2] Beil I, Hiskens I, Backhaus S. Frequency regulation from commercial building HVAC demand response. *Proc IEEE* 2016;104(4):745–57.
- [3] Zhang N, Kang C, Xia Q, Liang J. Modeling conditional forecast error for wind power in generation scheduling. *IEEE Trans on Power Systems* 2014;29(3):1316–24.
- [4] Zhao Y, Noori M, Tatari O. Vehicle to Grid regulation services of electric delivery trucks: Economic and environmental benefit analysis. *Appl Energy* 2016;170:161–75.
- [5] Ding Y, Shao C, Yan J, Song Y, Zhang C, Guo C. Economical flexibility options for integrating fluctuating wind energy in power systems: The case of China. *Appl Energy* 2018;228:426–36.
- [6] Wang J, Zhong H, Ma Z, Xia Q, Kang C. Review and prospect of integrated demand response in the multi-energy system. *Appl Energy* 2017;202:772–82.
- [7] Kuzlu M, Pipattanasomporn M, Rahman S. Hardware demonstration of a home energy management system for demand response applications. *IEEE Trans on Smart grid* 2012;3(4):1704–11.
- [8] Residential energy consumption survey (RECS). < <https://www.eia.gov/consumption/residential/reports/2015/overview/> >; 2018, 5.
- [9] Zhang C, Xue X, Zhao Y, Zhang X, Li T. An improved association rule mining-based method for revealing operational problems of building heating, ventilation and air conditioning (HVAC) systems. *Appl Energy* 2019;253:113492. <https://doi.org/10.1016/j.apenergy.2019.113492>.
- [10] Kim YJ, Blum DH, Xu N, Su L, Norford LK. Technologies and Magnitude of Ancillary Services Provided by Commercial Buildings. *Proc IEEE* 2016;104(4):758–79.
- [11] Ding Y, Cui W, Zhang S, Hui H, Qiu Y, Song Y. Multi-state operating reserve model of aggregate thermostatically-controlled-loads for power system short-term reliability evaluation. *Appl Energy* 2019;241:46–58.
- [12] Braun J, Montgomery K, Chaturvedi N. Evaluating the performance of building thermal mass control strategies. *HVAC&R Research* 2001;7(4):403–28.
- [13] Wang H, Wang S, Tang R. Development of grid-responsive buildings: Opportunities, challenges, capabilities and applications of HVAC systems in non-residential buildings in providing ancillary services by fast demand responses to smart grids. *Appl Energy* 2019;250:697–712.
- [14] Xie D, Hui H, Ding Yi, Lin Z. Operating reserve capacity evaluation of aggregated heterogeneous TCLs with price signals. *Appl Energy* 2018;216:338–47.
- [15] Fu Y, Lu Z, Hu W, Wu S, Wang Y, Dong L, et al. Research on joint optimal dispatching method for hybrid power system considering system security. *Appl Energy* 2019;238:147–63.
- [16] Winstead C, Bhandari M, Nutaro J, Kuruganti T. Peak load reduction and load shaping in HVAC and refrigeration systems in commercial buildings by using a novel lightweight dynamic priority-based control strategy. *Appl Energy* 2020;277:115543. <https://doi.org/10.1016/j.apenergy.2020.115543>.
- [17] Qi Y, Wang D, Jia H, et al. Demand response control strategy for central air-conditioner based on temperature adjustment of partial terminal devices. *Automation of Electric Power Systems* 2015;39(17):82–8.
- [18] Hui H, Ding Y, Liu W, Lin Y, Song Y. Operating reserve evaluation of aggregated air conditioners. *Appl energy* 2017;196:218–28.
- [19] Hui H, Siano P, Ding Y, et al. A transactive energy framework for inverter-based HVAC loads in a real-time local electricity market considering distributed energy resources. *IEEE Trans Ind Inform* 2022; Early Access, <https://doi.org/10.1109/TII.2022.3149941>.
- [20] Motegi N, Piette MA, Watson DS, et al. Introduction to commercial building control strategies and techniques for demand response. Lawrence Berkeley National Laboratory LBNL-59975 2007.
- [21] Guiyin F. Energy storage air conditioning technology. Machinery Industry Press 2006.
- [22] Blum DH, Norford LK. Dynamic simulation and analysis of ancillary service demand response strategies for variable air volume HVAC systems. *HVAC&R RESEARCH* 2014;20(8):908–21.
- [23] Berardino J, Nwankpa C. Dynamic Load modeling of an HVAC chiller for demand response applications. In: First IEEE International Conference on Smart Grid Communications. 2010.
- [24] Hong J, Hui H, Zhang H, Dai N, Song Y. Distributed control of large-scale inverter air conditioners for providing operating reserve based on consensus with nonlinear protocol. *IEEE Internet Things J* 2022; Early Access, <https://doi.org/10.1109/JIOT.2022.3151817>.
- [25] Yao L, Lu H-R. A two-way direct control of central air-conditioning load via the internet. *IEEE Trans on Power Delivery* 2009;24(1):240–8.
- [26] Yao L, Damiran Z, Lim W. H. Direct load control of central air conditioning systems using fuzzy optimization. In: 2016 IEEE 16th International Conference on Environment and Electrical Engineering (EEEIC); 2016.
- [27] Cui W, Ding Y, Hui H, Lin Z, Du P, Song Y, et al. Evaluation and sequential dispatch of operating reserve provided by air conditioners considering lead-lag rebound effect. *IEEE Trans on Power Systems* 2018;33(6):6935–50.
- [28] Wang B, Zhu F, Ji W, et al. Load cutting potential modeling of central air-conditioning and analysis on influencing factors. *Automation of Electric Power Systems* 2016;40(19):44–52.
- [29] Su L, Norford LK. Demonstration of HVAC chiller control for power grid frequency regulation—Part 1: Controller development and experimental results. *Science and Technology for the Built Environment* 2015;21(8):1134–42.
- [30] Sivaneasan B, Kandasamy NK, Lim ML, Goh KP. A new demand response algorithm for solar PV intermittency management. *Appl energy* 2018;218:36–45.
- [31] Blum DH, Xu N, Norford LK. A novel multi-market optimization problem for commercial heating, ventilation, and air-conditioning systems providing ancillary services using multi-zone inverse comprehensive room transfer functions. *Science and Technology for the Built Environment* 2016;22(6):783–97.
- [32] Wang S, Tang R. Supply-based feedback control strategy of air-conditioning systems for direct load control of buildings responding to urgent requests of smart grids. *Appl Energy* 2016;201(sep.1):419–32.
- [33] Tang R, Wang S. Model predictive control for thermal energy storage and thermal comfort optimization of building demand response in smart grids. *Appl Energy* 2019;242:873–82.
- [34] Xie K, Hui H, Ding Y. Review of modeling and control strategy of thermostatically controlled loads for virtual energy storage system. *Protection and Control of Modern Power Systems* 2019;4(1):1–13.
- [35] Wan JW, Zhang WJ, Zhang WM. An energy-efficient air-conditioning system with an exhaust fan integrated with a supply fan. *Energy Build* 2009;41(12):1299–305.
- [36] Blum DHDH. Analysis and characterization of ancillary service demand response strategies for variable air volume HVAC systems. Massachusetts Institute of Technology 2013.
- [37] Cheng L, Wan Y, Tian L, Zhang F. Evaluating energy supply service reliability for commercial air conditioning loads from the distribution network aspect. *Appl Energy* 2019;253:113547. <https://doi.org/10.1016/j.apenergy.2019.113547>.
- [38] U.S. DOE, EnergyPlus Manual, Version 2.2; 2008.
- [39] Modelica Buildings Library. < <https://simulationresearch.lbl.gov/modelica/>>.
- [40] Wang D, Zhang G, Jing Y, Liu M, Li J, Cheng D. Control of central air conditioning loads to respond the fault on the HVDC transmission line. *The Journal of Engineering* 2019;2019(16):2266–70.
- [41] Liu M, Guo Q, Zhang G, Su J. Application of emergency control of central air conditioning in safe and stable operation of large power grid. *The Journal of Engineering* 2019;2019(16):1539–43.
- [42] Liu F, Guan G, Xin J. Applicability of Temperature Set-Point Regulation on Commercial Air Conditioners in Power Systems with Various Load Characteristics. In: 2018 IEEE/PES Transmission and Distribution Conference and Exposition (T&D). 2018.
- [43] Hui H, Ding Y, Lin Z, Siano P, Song Y. Capacity allocation and optimal control of inverter air conditioners considering area control error in multi-area power systems. *IEEE Trans on Power Systems* 2020;35(1):332–45.